Ocean Sci. Discuss., 11, 2367–2389, 2014
www.ocean-sci-discuss.net/11/2367/2014/
doi:10.5194/osd-11-2367-2014

Ocean Science
Discussions
Open Access

Wind increase above warm Agulhas Current eddies

M. Rouault[1,2], **P. Verley**[1,3], **and B. Backeberg**[1,2,4]

[1]Department of Oceanography, MA-RE Institute, University of Cape Town, Rondebosch, South Africa
[2]Nansen-Tutu Center for Marine Environmental Research, University of Cape Town, Rondebosch, South Africa
[3]ICEMASA, UMR EME, IRD, Centre de Recherche Halieutique Méditerranéenne et Tropicale, Sète, France
[4]Nansen Environmental and Remote Sensing Centre, Bergen, Norway

Received: 8 September 2014 – Accepted: 21 September 2014 – Published: 21 October 2014

Correspondence to: M. Rouault (mathieu.rouault@uct.ac.za)

Published by Copernicus Publications on behalf of the European Geosciences Union.

Abstract

Sea surface temperature estimated from the Advanced Microwave Scanning Radiometer E onboard the Aqua satellite and altimetry derived sea level anomalies are used south of the Agulhas Current to identify warm mesoscale eddies presenting a distinct SST perturbation superior to 1 °C to the surrounding ocean. The analysis of 2500 instantaneous charts of equivalent stability neutral wind speed estimates from the SeaWinds scatterometer onboard the QuikScat satellite collocated with sea surface temperature and sea level anomaly show stronger wind speed above warm eddies than surrounding water at all wind directions in about 800 of the 2500 cases. For those cases where the wind is stronger above warm eddies, we do not find any relationship between the increase in surface wind speed and the sea surface temperature perturbation. Sea surface temperature perturbations that we consider range from 1 to 5.5 °C. Sizes of eddies range from 100 to 250 km diameter. Mean background wind speed is about 11 m s^{-1} with a mean increase above the eddy of 2 m s^{-1}. Wind speed increase of 4 to 7 m s^{-1} above warm eddies is not uncommon.

1 Introduction

Microwave radiometry and altimetry allow making observations in the Southern Ocean with unprecedented spatial and temporal resolution. Clouds and water vapor do not inhibit sea surface temperature (SST) estimated by the Advanced Microwave Scanning Radiometer E (AMSR-E) onboard the Aqua satellite. This is a real advantage in the latitudes between 35 to 50° S south of Africa where persistent cloud cover previously was a perennial problem in this regard. Furthermore, the merging of measurements by several altimeters flying on TOPEX/Poseidon satellite, European Research Satellite 2 and Jason-1 satellite allows a better description of mesoscale ocean features in highly energetic regions (Ducet et al., 2000). In addition, equivalent stability neutral instantaneous wind speed estimates from the SeaWinds scatterometer onboard the

OSD
11, 2367–2389, 2014

QuikScat satellite is available from July 1999 (Chelton et al., 2004) to November 2009 at a quarter of a degree resolution along a wide swath.

The latter product, combined with SST estimates from the Tropical Microwave Imager (TMI) onboard the Tropical Rainfall Measuring Mission (TRMM), allowed to demonstrate the impact of mesoscale oceanic features on the overlying atmosphere (Xie, 2004; Chelton and Wentz, 2005). Chelton et al. (2000) and Hashizume et al. (2001) have combined wind stress estimates from QuikScat and TMI SST in the eastern tropical Pacific to study the impact on the atmosphere of tropical instability waves, oceanic features with periods of 20 to 40 days and wavelengths of 1000–2000 km. Chelton et al. (2004) used 4 years of filtered QuikScat data to show a ubiquitous picture of mesoscale ocean atmosphere interaction linked to SST heterogeneity such as fronts, western boundary currents and tropical instability waves. TMI SST, QuikScat wind speed estimate and in situ observation were also used by Nonaka and Xie (2003) to reveal SST and wind speed covariability over the Kuroshio Extension east of Japan. In general, using satellite estimates of wind speed, wind stress and SST, there is a linear relationship between SST perturbation and wind speed or wind stress especially evident for SST perturbation from the surrounding ocean between −1 and 1 °C. However, no linear relationship was found by Park et al. (2006) between change in wind speed and wind stress curl and SST perturbation higher than 1 °C across Gulf Stream eddies.

Closer to Africa, White and Annis (2003) used low pass filtered altimetry derived sea level height, SST and QuikScat meridional wind speed for periods superior to 1 month and for zonal wavelengths of 400–1200 km in the Agulhas Current system and they illustrated a coupling between mesoscale eddies and westerly wind. O'Neill et al. (2005) used filtered monthly AMSR-E SST and QuikScat data to show that the wind stress increases and decreases as it goes over warm and cold meanders of the Agulhas Return Current. Filtering the data on a large domain, they found a linear relationship between SST perturbation and wind stress. Rouault and Lutjeharms (2000) measured high values of latent and sensible heat fluxes above a warm eddy south of the Agulhas Current

OSD
11, 2367–2389, 2014

during the SAAMES 3 cruise in June 1993 and they presented a clear homogeneous increase in wind speed estimate from the ERS-1 satellite above this warm eddy that was presenting a 6 °C perturbation with surrounding ocean.

Several mechanisms can explain the phenomena that encompass a high range of SST (from 12 to 30 °C) and wind speed (from low to high wind speed) and were comprehensively reviewed by Small et al. (2008). It is thought that the increase or decrease of surface wind speed along SST gradient is due to the change in the latent and sensible turbulent heat fluxes and associated change in surface atmospheric stability. Consequently there is a substantial modification of the constant flux layer and of the height and structure of the marine atmospheric boundary layer above the surface layer. According to the numerical study of Samelson et al. (2006) this creates a change in atmospheric conditions leading to the observed wind speed increase or decrease at the surface. Another possible effect is that change in the stability parameter of the constant flux layer at the surface lead to a modification of the logarithm profile that characterizes wind speed, temperature and humidity in the surface layer. This increases the downward mixing of momentum (Wallace et al., 1989) leading to the wind speed increase. The change in pressure along SST gradient is also thought to drive secondary circulations (Wai and Stage, 1989; Cronin et al., 2003).

Figure 1 shows the mean SST in August 2003 south of Africa done using AMSR-E SST. The Agulhas Current can be seen to follow the eastern coastline of South Africa closely (temperatures exceeding 18 °C) and seems to be in the process of shedding a ring at 37° S, 17° E. Two well-defined warm eddies with temperatures of about 16–17 °C are evident at about 40° S, 15° E and 42° S, 24° E. They create an important gradient in SST with the surrounding ocean. The meanders of the Agulhas Return Current, object of O'Neill et al.'s study (2005) and Liu et al. (2007), are also evident along 39° S from 25° E eastwards.

The Agulhas Retroflection has an average loop diameter of 340 km and can be found between 16 and 20° E (Lutjeharms and van Ballegooyen, 1988). On average, five anticyclonic rings are shed each year from the occlusion of the retroflection loop (Schouten

OSD
11, 2367–2389, 2014

et al., 2000) and move in a northwestward direction into the South Atlantic Ocean (Byrne et al., 1995; Schouten et al., 2000). Apart from Agulhas a ring, a number of other eddies are also formed in this region. Lutjeharms and Valentine (1988) observed eddies with a range of sizes at the termination of the Agulhas retroflection loop. Particularly evident are warm eddies shed southward across the Subtropical Convergence into the colder waters of the subantarctic.

Unlike rings those eddies offer high SST gradients leading to a five-fold increase of the latent and sensible heat flux (Rouault and Lutjeharms, 2000; Rouault and Lee-Thorp, 1996). Those eddies were chosen because they offer a very distinct SST contrast with surrounding water of up to six degrees, they move slowly and can be considered almost stationary at the weekly scale. Due to their high heat content and depth, it takes a few months before they loose their surface expression in temperature. At last, we conducted air sea interaction measurements in similar eddies in 1993 (Rouault and Lutjeharms, 2000) that provide observational insights.

The objective of our study is to explore the interaction between the atmosphere and warm eddies with a clear surface expression (SST perturbation $> 1\,^{\circ}$C) for a variety of wind directions and SST perturbation to directly quantify the effect of the SST perturbation on wind speed without filtering the data. Eddies were identified with a combination of AMSR-E SST and altimetry. Twice daily instantaneous gridded wind speed estimates from QuikScat were examined above six warm eddies (Sect. 3) for a period of two years and a quantification of the effect of SST perturbation on wind speed increase above those warm eddies was conducted. At last, we discussed possible reasons for why we do not find a linear relationship between the increase in surface wind speed and high SST perturbation.

2 Data

SST was derived from the AMSR-E, launched in 2002 by NASA. It is a passive microwave radiometer with 6 frequencies that measures brightness temperature at

OSD
11, 2367–2389, 2014

Title Page
Abstract | Introduction
Conclusions | References
Tables | Figures
◀| |▶
◀ ▶
Back | Close
Full Screen / Esc
Printer-friendly Version
Interactive Discussion

6.9 GHz, for a 90 % complete global ground coverage within a day, with an accuracy of 0.4 K (Chelton and Wentz, 2005). In this investigation, we use weekly data produced by the Remote Sensing System at a resolution of 56 km. We used twice daily equivalent stability neutral surface instantaneous wind speed and direction estimated by the Sea-Winds scatterometer on the QuikScat satellite. It is QuikSCAT Level 2B Ocean Wind Vectors in 25 Km Swath Grid. Weekly sea level anomalies (SLA) and geostrophic current were obtained from Centre national d'études spatiales (CNES). They are given on a one third of a degree grid (Ducet et al., 2000). They are based on merged observation of the TOPEX/Poseidon, the European Research Satellite 2 (ERS-2) and the Jason-1 altimeters. We took as an eddy definition a SLA of +15 cm. However, the intense mesoscale variability in SLA generated at the Agulhas Retroflection and in the Agulhas Return Current, make the observation of eddies using satellite altimetry only somewhat ambiguous. This is especially true near the shifting or meandering current. However, the combined use of SST and altimetry allows one to identify eddies with less ambiguity than with altimetry alone. The selected eddies shed from the Agulhas Retroflection and the Agulhas Return Current, were identified in an area ranging from 35 to 45° S latitude and 15 to 25° E longitude. There are presented in Fig. 2. For most of the cases, the period of unambiguous observation therefore does not exceed a couple of months but for some it exceeds a year. In fact most eddies that we were interested in stayed quite close to the Agulhas Return Current for a few months and were reabsorbed by the Agulhas Retroflection or the Agulhas Return Current. AMSR-E SST was therefore instrumental in corroborating the location of warm eddies and their trajectories.

3 Eddy detection

Our period of study was July 2002–June 2004 and the geographic domain of the study is defined by Fig. 1. Using SST and altimetry data in this region, we selected warm eddies that had a significantly different surface thermal expression at the sea surface compared to ambient waters. The first eddy, Eddy1, was shed off warm water moving

OSD
11, 2367–2389, 2014

westward through the Agulhas Retroflection in June 2002 at about 16° E–41° S. The eddy had an observed SLA of about +30 cm during the five first months of its existence. Its diameter was an estimated 130 km. During its first month, the eddy moved southward to 15° E, 44° S. By mid-July 2002 the surface temperature of the eddy core was over 14 °C, and distinctly warmer than the surrounding water that was 8 to 10 °C. For the analysis of the influence of this eddy on the atmosphere, we focused on the periods when the eddy presented significant SST gradients in July and August 2002. The second eddy, Eddy2 was shed from the Agulhas Return Current in mid-July 2002 at 24° E, 42° S. The shedding was not fully complete until the end of August 2002. The maximum SLA observed was about +90 cm with a 4 °C temperature difference between the edge and the core of the eddy. At the end of October, Eddy 2 seemed to have merged with another eddy. The period of study for this eddy is September to November 2002. Eddy3 formed as a small eddy at the Agulhas Retroflection around mid-January 2003 at 17° E, 43° S, with a maximum SLA of 20 cm and a diameter of about 200 km. The eddy moved rapidly southwestward to reach 15° E, 44.5° S at the end of March 2003. The temperature difference between the edge of the eddy and its core was about 3 °C. By mid-April 2003, the SST expression of the eddy had disappeared. The period of observation for the third eddy is February and March 2003. The fourth eddy was shed from the retroflection in the first week of July 2003 at 15° E, 40° S. The SLA at the center of the eddy was about 65 cm and the diameter was estimated to be 250 km. The eddy had a maximum SST of over 16 °C at its core. The surrounding water temperature was between 12 to 14 °C. At the beginning of September 2003, the eddy was re-integrated with the current. Eddy 4 presented a strong gradient of temperature with the surrounding ocean in July and August 2003 and in many respects was similar to the eddy surveyed intensively in June and July 1993 by Rouault and Lutjeharms (2000). The period of observation for this eddy is July and August 2003. Eddy 5 had been shed mid-June 2003 at 24° E, 41° S with a maximum SLA of 80 cm. The SST ranged from 12 °C at the edge to 16 °C at the center of the feature. The eddy barely moved during the next four months. At the beginning of November 2003, there

OSD
11, 2367–2389, 2014

remained no distinctive SST gradient between the eddy and surrounding waters and it became reattached to the Agulhas Retroflection a few weeks later. This eddy had a well defined SST expression that lasted from July to October 2003. Eddy 6 was shed from the Agulhas Retroflection the last week of December 2003. At the end of December 2003, the eddy was about 230 km in diameter and centered on 16° E, 41° S, with an observed maximum SLA of 75 cm. It was clearly separated from the Agulhas Current at the end of January 2004 at 15° E, 43° S and exhibited a strong gradient with the surrounding ocean. The SST of the eddy was 18 °C at its core and 10 °C at the edge. It took about one year for the distinct SST expression of the eddy to vanish by which time the temperature of the core had reached the 8 to 10 °C of the surrounding water. The eddy SSH was still present at the end of July. Eddy 6 was then located at 12° E, 41° S. The period of observation for Eddy 6 was from February to June 2004.

4 Wind speed acceleration above eddies

As described above, for the two year period from 2 July 2002 to 2 June 2004, we selected 6 warm eddies south of Africa that presented strong surface thermal contrasts with the surrounding ocean. Such eddies were found in an area between 35 to 45° S latitude and 15 to 25° E longitude (Fig. 2). The record represents a total of 22 months of clear-cut, identifiable eddies. We have cases for all seasons with a variety of SST (19 to 12 °C) and SST perturbations of up to 5.5 °C. Figure 3 shows 4 examples of scene showing high acceleration above warm eddies and deceleration over colder features. The Agulhas Current is found to the North of the domain. In the four selected cases, wind speed increase is superior to 6 m s^{-1} and relatively homogeneous above eddies. Next, we show in Fig. 4 shows a weekly average of the instantaneous wind speed and SST above the six eddies. Eddies are almost stationary at the weekly time scale. Times given correspond to weekly means centered at 10 July 2002 for Eddy 1, at 4 September 2002 for Eddy 2, at 19 March 2003 for Eddy 3, at 16 July 2007 for Eddy 4, at 3 September 2003 for Eddy 5 and at 5 may 2004 for Eddy 6. Wind is mostly westerly

OSD
11, 2367–2389, 2014

at the weekly scale, a common feature of the “Roaring Forties”. Figure 4 shows an increase in wind speed ranging from 2 to 5 $\mathrm{m\,s^{-1}}$ above all the eddies at the weekly scale. As discussed later, all instantaneous morning and evening paths do no display a clear increase above eddies but it is enough to have a strong imprint on the wind field at that scale.

A month of the twice daily QuikScat instantaneous wind speed above eddy 5 in July 2003 averaged for four main wind directions is presented in Fig. 5. We have separated the data according to 4 directional quadrants (West, North, East, and South) and vector averaged the result. In July 2003, the westerly selection provided 36 cases, the northerly, 18, the easterly, 1 and the southerly wind, 6. Missing data for the easterly case results from rain interference. Wind speed shows clear increases above the eddy for all directions of the wind. The wind strengthening is substantial with an increase from about 10 to 15 $\mathrm{m\,s^{-1}}$ across the eddy. The wind seems also to react rapidly to all features that create a SST gradient, for instance, the Agulhas Retroflection to the north. Air masses coming from the north had already been modified by high latent and sensible heat fluxes above the Agulhas Current (Rouault et al., 2000) yet the wind speed clearly decrease after the Agulhas Current and then increases again above the eddies.

We then systematically plotted the SeaWinds wind speed and direction for morning and evening passes with corresponding weekly SST and SLA for a period of two years and examined those 1460 charts. SST and SLA were interpolated into the two year long two-daily wind speed dataset. Because some months had two eddies at a time we ended up with about 2500 cases. Increase in wind speed above warm eddies and decrease downwind were a clear feature for 35 % of the cases. However, for about 65 % of the cases there were no clear increases above those warm eddies. For those cases, the weather patterns were usually dominated by frontal conditions associated with low pressure systems. In many of the scenes where the SST seems to have had no effect on the winds over eddies, the wind pattern was representative of powerful cyclonic systems. 10 % of the scenes were contaminated with rainfall or had no data.

OSD
11, 2367–2389, 2014

This left us with about 800 cases with a clear homogeneous increase above eddies and decrease downwind of eddies.

To quantify the relationship between SST perturbation, wind speed increase, season and eddy duration we looked at the statistics of the merged dataset of those 800 cases that presented a clear homogeneous increase and a SST perturbation > 1 °C. For each scene, we extracted SST, SLA, absolute geostrophic current and wind speed at three positions along the wind flow: (a) before the border of the eddy in undisturbed condition (b) in the middle of the eddy (c) downwind of the eddy border. SST and wind speed gradient was calculated across the eddy border at the entrance of the flow. Figure 6 presents a scatter plot of the instantaneous wind speed increase DW vs. the SST perturbation DSST. Wind speed increase of up to 7 $\mathrm{m\,s^{-1}}$ are evident in our dataset with a great number of case showing increase superior to 2 $\mathrm{m\,s^{-1}}$ well above the range of error due to the use of stability neutral wind speed. For those 800 scenes, the mean increase was about 2 $\mathrm{m\,s^{-1}}$ for a mean wind speed of 11 $\mathrm{m\,s^{-1}}$ at the entrance, slightly higher than Park et al. (2006) study of wind speed modification across Gulf Stream eddies who found an increase of about 10 to 15 %. Most of selected wind speed background ranged between 5 and 20 $\mathrm{m\,s^{-1}}$. The eddy SST centers ranged from 19 to 12 °C with SST perturbation of up to 5.5 °C for a mean gradient of 2.5 °C per 100 km. This is substantially higher than values of wind speed increase and SST perturbation given in White and Amis (2003) for the region using filtered data. They found an average increase of 1.2 $\mathrm{m\,s^{-1}}$ for an average SST perturbation of 0.8 °C. Figure 6 does not show any clear linear relation between those parameters for perturbation > 1. This seems to contradict a number of studies, although most where done for perturbation between 1 and −1. For instance, O'Neil et al. (2005) filtered monthly QuikScat and SST data in their study of wind stress acceleration and deceleration over the Agulhas Return Current and they found a linear relation between SST perturbation and wind speed increase (or decrease). We note that the filtering used by O'Neil et al. (2005) seems to underestimate the high SST gradients experienced in the Agulhas Current system as most of their cases have SST perturbation between −1 and 1 which is clearly too low

OSD
11, 2367–2389, 2014

(Rouault and Lee-Thorp, 1996; Lee-Thorp et al., 1999; Rouault and Lutjeharms, 2000; Rouault et al., 1995, 2000).

5 Discussion

A caveat in all those study of wind increase or decrease above sea surface temperature front is that QuikScat wind speeds were not calibrated for unstable or stable conditions but for neutral condition. Those conditions occur above warm Agulhas eddy or Agulhas Current at low wind speed (Rouault and Lee-Thorp, 1996; Lee-Thorp et al., 1999; Rouault et Lutjeharms, 2000; Rouault et al., 1995, 2000). This critic applies to many papers mentioned in the introduction or in the review by Small et al. (2008). For instance, the difference at 10 m between neutral and unstable condition for a 7 m s^{-1} wind speed, relative humidity of 75 %, SST of 20 °C and air temperature of 18 °C is 0.5 m s^{-1} (Liu et al., 2007; Fig. 1). Wai and Stage (1989) and O'Neill et al. (2005) considered that this effect is small compared to the overall observed increase in wind speed discussed here. In our study we note that because we have quite strong wind speed here (mean of 11 m s^{-1}) the conditions are generally near neutral. Another potential problem is the resolution of the data used (56 km for SST and about 30 km for wind speed). For instance measured SST perturbation for an eddy similar to eddy 5 was 6 °C across 50 km (Rouault and Lutjeharms, 2000) while our stronger perturbation is 5.5 °C, a twofold underestimation of the SST gradient. Park et al. (2006) using high resolution SST data calculated SST gradients across Gulf Stream eddies of up to 2.5 °C (10 km)$^{-1}$, an effect underestimated by the filtering done by White and Amis (2003); Chelton et al. (2004) and Small et al. (2008) in the Gulf Stream region. Park et al. (2006) clearly show that for strong SST perturbation the linear relationship between SST perturbation and wind speed change or wind stress curl change does not hold (Figs. 11, 12 and 16 in Park et al., 2006).

OSD
11, 2367–2389, 2014

Another caveat was discussed by Grodski et al. (2012) who found an impact of SST on short wind waves and sea roughness not taken into account in algorithms that are used to estimate wind speed or wind stress with satellite remote sensing signal.

The reason for the absence of linearity between wind speed increase and SST perturbation could mean that the observed increase is not a direct function of the high turbulent fluxes of latent and sensible heat and the associated stability parameter. It may be that the increase in wind speed is due to change in the height of the boundary layer (Samelson et al., 2006) or the pressure gradient (Wai and Stage, 1989; Cronin et al., 2003). It maybe a combination of those 3 factors. Or, this could mean that the algorithm used to infer the wind speed is not adequate for those situations of high SST gradient and unstable conditions.

We note that the wind speed increase on average by about 15 % with quite a number of case above 3 $m\,s^{-1}$. This is quite substantial to be explained by surface layer and logarithmic profiles consideration. We recall that the logarithmic profile of wind speed in the boundary layer is a function of the stability parameters. The stability parameter is analogous to the Richardson number, which is the ratio of the work done by the buoyant force to the rate of shear production of turbulent energy. It takes into account both the temperature and moisture dependence of air parcel buoyancy and is affected by the friction velocity. The stability influences the vertical exchange of energy and momentum and thereby the vertical distribution of wind speed, temperature and humidity in the boundary layer. A positive number of the stability means that the conditions are stable and the stratification will act against the turbulence. Between 0 and −0.3 the stability is neutral. If the stability is less than −0.3 the conditions are unstable with convective activity: the buoyant force begins to dominate the mixing process. Rouault and Lutjeharms (2000) presents time series of those parameters above a 16 °C similar eddies to those studied here. Conditions were neutral or near neutral during the week spend above the eddy during the SAAMES 3 cruises. Only when the wind speed dropped below 5 $m\,s^{-1}$ that conditions became clearly unstable.

OSD
11, 2367–2389, 2014

Another possible reason for the non-linearity concerns the impact of the marine atmospheric boundary layer height on wind speed increase, an effect modeled by Samelson et al. (2006) who conclude that the change in stability at the surface is not enough to create the observed increase. Indeed large changes in the height of the MABL were observed in the region by Liu et al. (2007) using satellite remote sensing or were measured with radiosondes (Lee-Thorp et al., 1998, 1999; Rouault and Lee-Thorp, 1996; Rouault et al., 1995, 2000). The high turbulent fluxes and mixing can modify substantially the height and structure of the marine atmospheric boundary layer above the surface layer and create a change in atmospheric conditions leading to the observed wind speed increase and decrease Samelson et al. (2006). This effect will take longer to take place than the modification of the logarithm profile in the constant flux layer (Park et al., 2006) and may need high latent and sensible fluxes.

A third effect already mentioned concern the pressure gradient. To summarize it maybe that these three effects are at work and because they have different time and spatial scale this lead to no linear relationship between SST perturbation and wind speed increase for SST perturbation superior to 1 °C.

6 Conclusions

Modifications to the marine atmospheric boundary layer and ocean–atmosphere interaction across frontal regions were documented during experiments at sea (Sweet et al., 1981; Davidson et al., 1991; Friehe et al., 1991; Rouault et al., 2000; Bourras et al., 2004) and also modelled (Samelson et al., 2006; Bourras et al., 2004). Satellite remote sensing confirms and extends in space and time the relationship demonstrated during those experiments. Wind speed, wind stress and turbulent fluxes and latent and sensible heat increase substantially when crossing positive SST gradient. Using microwave remote sensing from satellite has been beneficial in this regard, as it provides a full global coverage of the Southern Ocean. A combination of merged SLA, geostrophic velocity and microwave SST is a very useful tool for studying the path and track of

OSD
11, 2367–2389, 2014

eddies. This could be displayed operationally to provide vessels with early warning and to indicate where there are likely to sustain stronger wind. With increases of more than $4\,m\,s^{-1}$ in eddies not uncommon, the warning should be taken seriously when sailing in the "Roaring Forties". At last this study seriously questions the hypothesis that there is a linear relationship between SST gradient and wind speed increase or decrease for large SST perturbation > 1 °C. As those conditions occur in all western boundary current systems or in upwelling region areas, there is a need to calibrate remote sensed wind stress and wind speed estimate for unstable and stable condition and to account for SST in algorithm used to infer wind stress, wind speed and wind stress curl from backscatter signal. This call for a dedicated experiment and the deployment of two moorings in area of strong SST gradient.

Acknowledgements. Mathieu Rouault wishes to thank ESA GlobeCurrent project, ACCESS, NRF, the Nansen-Tutu Center for Marine Environmental Research and the South African Water Research Commission for financial support. AMSR-E and twice daily wind data were produced by Remote Sensing Systems, http://www.ssmi.com, and sponsored by NASA's Earth Science Information Partnerships (ESIP): a federation of information sites for Earth Science; and by NASA's TRMM Science Team. Thanks to AVISO, CNES and CLS for making the T/P ERS JASON merged product available.

References

Bourras, D., Reverdin, G., Giordani, H., and Caniaux, G.: Response of the atmospheric boundary layer to a mesoscale oceanic eddy in the northeast Atlantic, J. Geophys. Res., 109, D18114, doi:10.1029/2004JD004799, 2004.

Byrne, D. A., Gordon, A. L., and Haxby, W. F.: Agulhas Eddies: a synoptic view using Geosat ERM data, J. Phys. Oceanogr., 25, 902–917, 1995.

Chelton, D. B. and Wentz, F. J.: Global high-resolution satellite observations of sea-surface temperature for numerical weather prediction and climate research, B. Am. Meteorol. Soc., 86, 1097–1115, 2005.

Chelton, D. B., Wentz, F. J., Gentemann, C. L., de Szoeke, R. A., and Schlax, M. G.: Satellite microwave SST observations of transequatorial tropical instability waves, Geophys. Res. Lett., 27, 1239–1242, 2000.

Chelton, D. B., Esbensen, S. K., Schlax, M. G., Thum, N., Freilich, M. H., Wentz, F. J., Gentemann, C. L., McPhaden, M. J., and Schopf, P. S.: Observations of coupling between surface wind stress and sea surface temperature in the Eastern Tropical Pacific, J. Climate, 14, 1479–1498, 2001.

Chelton, D. B., Schlax, M. G., Freilich, M. H., and Milliff, R. F.: Satellite measurements reveal persistent small-scale features in ocean winds, Science, 303, 978–983, 2004.

Cronin, M. F., Xie, S.-P., and Hashizume, H.: Barometric pressure variations associated with eastern Pacific tropical instability waves, J. Climate, 16, 3050–3057, 2003.

Davidson, K. L., Boyle, P. J., Gautier, C., Hanson, H. P., and Khalsa, S. J. S.: Medium- to large-scale atmospheric variability during the Frontal Air–Sea Interaction Experiment, J. Geophys. Res., 96, 8531–8551, 1991.

Ducet, N., Le Traon, P.-Y., and Reverdin, G.: Global high resolution mapping of ocean circulation from TOPEX/Poseidon and ERS-1/2, J. Geophys. Res., 105, 19477–19498, 2000.

Friehe, C. A., Shaw, W. J., Rogers, D. P., Davidson, K. L., Large, W. G., Stage, S. A., Crescenti, G. H., Khalsa, S. J. S., Greenhut, G. K., and Li, F.: Air–sea fluxes and surface layer turbulence around a SST front, J. Geophys. Res., 96, 8593–8609, 1991.

Grodsky, S. A., Kudryavtsev, V. N., Bentamy, A., Carton, J. A., and Chapron, B.: Does direct impact of SST on short wind waves matter for scatterometry?, Geophys. Res. Lett., 39, L12602, doi:10.1029/2012GL052091, 2012.

Hashizume, H., Xie, S.-P., Liu, W. T., and Takeuchi, K.: Local and remote atmospheric response to tropical instability waves: a global view from space, J. Geophys. Res., 106, 10173–10185, 2001.

Lee-Thorp, A. M., Rouault, M., and Lutjeharms, J. R. E.: Cumulus cloud formation above the Agulhas Current, S. Afr. J. Sci., 94, 351–354, 1998.

Lee-Thorp, A. M., Rouault, M., and Lutjeharms, J. R. E.: Moisture uptake in the boundary layer above the Agulhas Current: a case study, J. Geophys. Res., 104, 1423–1430, 1999.

Liu, T. W., Xie, X., and Niiler, P. P.: Ocean–atmosphere interaction over Agulhas Extension Meanders, J. Climate, 20, 5784–5797, doi:10.1175/2007JCLI1732.1, 2007.

Lutjeharms, J. R. E. and Valentine, H. R.: Eddies at the sub-tropical convergence south of Africa, J. Phys. Oceanogr., 18, 761–774, 1988.

OSD
11, 2367–2389, 2014

Lutjeharms, J. R. E. and van Ballegooyen, R. C.: The retroflection of the Agulhas Current, J. Phys. Oceanogr., 18, 1570–1583, 1988.
Nonaka, M. and Xie, S.-P.: Covariations of sea surface temperature and wind over the Kuroshio and its extension: evidence for ocean-to-atmosphere feedback, J. Climate, 16, 1404–1413, 2003.
O'Neill, L. W., Chelton, D. B., Esbensen, S. K., and Wentz, F. J.: High-resolution satellite observations of SST modification of the marine atmospheric boundary layer over the Agulhas Return Current, J. Climate, 18, 2706–2723, 2005.
Park, K.-A., Cornillon, P. C., and Codiga, D. L.: Modification of surface winds near ocean fronts: effects of Gulf Stream rings on scatterometer (QuikSCAT, NSCAT) wind observations, J. Geophys. Res., 111, C03021, doi:10.1029/2005JC003016, 2006.
Rouault, M. and Lee-Thorp, A. M.: Fine-time resolution measurements of atmospheric boundary layer properties between Cape Town and Marion Island, S. Afr. J. Marine Sci., 17, 281–296, 1996.
Rouault, M. and Lutjeharms, J. R. E.: Air–sea exchange over an Agulhas eddy at the subtropical convergence, Global Atmosphere and Ocean System, 7, 125–150, 2000.
Rouault, M., Lee-Thorp, A. M., Ansorge, I., and Lutjeharms, J. R. E.: Agulhas Current air sea exchange experiment, S. Afr. J. Sci., 91, 493–496, 1995.
Rouault, M., Lee-Thorp, A. M., and Lutjeharms, J. R. E.: Observations of the atmospheric boundary layer above the Agulhas Current during alongcurrent winds, J. Phys. Oceanogr., 30, 70–85, 2000.
Samelson, R. M., Skyllingstad, E. D., Chelton, D. B., Esbensen, S. K., O'Neill, L. W., and Thum, N.: A note on the coupling of wind stress and sea surface temperature, J. Climate, 19, 1557–1566, 2006.
Schouten, M. W., de Ruijter, W. P. M., van Leeuwen, P. J., and Lutjeharms, J. R. E.: Translation, decay and splitting of Agulhas rings in the southeastern Atlantic Ocean, J. Geophys. Res., 105, 21913–21926, doi:10.1029/1999JC000046, 2000.
Small, R. J., DeSzoeke, S. P., Xie, S. P., O'Neill, L., Seo, H., Song, Q., Cornillon, P., Spall, M., and Minobe, S.: Air–sea interaction over ocean fronts and eddies, Dynam. Atmos. Oceans, 45, 274–319, 2008.
Sweet, W., Fett, R., Kerling, J., and LaViolette, P.: Air–sea interaction effects in the lower troposphere across the north wall of the Gulf Stream, Mon. Weather Rev., 109, 1042–1052, 1981.

OSD
11, 2367–2389, 2014

Wai, M. M. and Stage, S. A.: Dynamical analyses of marine atmospheric boundary layer structure near the Gulf Stream oceanic front, Q. J. Roy. Meteor. Soc., 115, 29–44, 1989.
Wallace, J. M., Mitchell, T. P., and Deser, C.: The influence of sea surface temperature on surface wind in the eastern equatorial Pacific: seasonal and interannual variability, J. Climate, 2, 1492–1499, 1989.
White, W. B. and Annis, J. L.: Coupling of extratropical mesoscale eddies in the ocean to westerly winds in the atmospheric boundary layer, J. Climate, 33, 1095–1107, 2003.
Xie, S.: Satellite observations of cool ocean–atmosphere interaction, B. Am. Meteorol. Soc., 85, 195–208, 2004.

OSD
11, 2367–2389, 2014

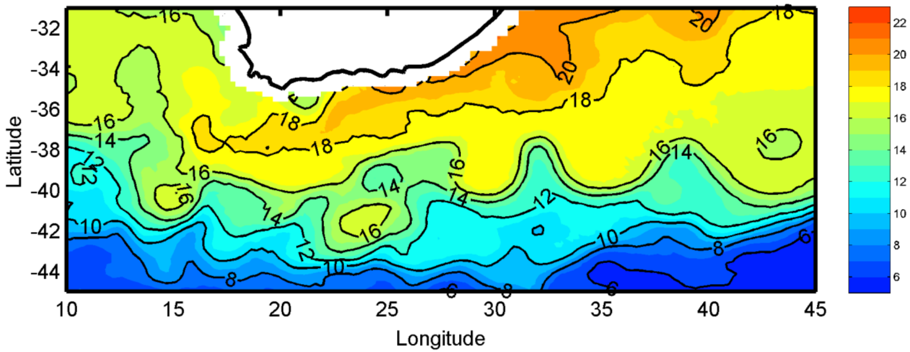

Figure 1. Mean SST in August 2003 for the region south of Africa, estimated with the Advanced Microwave Scanning Radiometer (AMSR-E) onboard the satellite Aqua. Two warm eddies with temperatures of about 16–17 °C can be seen centered on 40° S 15° E and 42° S 24° E. They create a strong SST gradient with the surrounding ocean. Cold eddies are visible at 38° S 43° E and at 39° S 25° E and an eddy is being shed from the Agulhas current at 37° S 17° E. The meanders of the Agulhas Return Current are also evident from 25° E eastward along 39° S.

OSD
11, 2367–2389, 2014

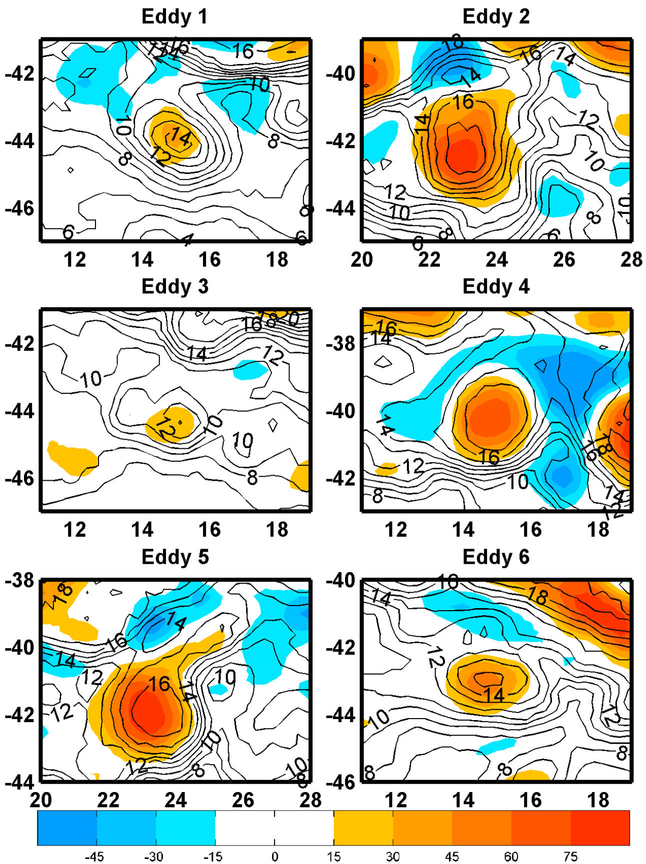

Figure 2. Mean weekly SST estimated from the AMSR-E and merged seal level anomaly for the 6 selected eddies. Times given correspond to weekly means centered at 10 July 2002 for Eddy 1, at 4 September 2002 for Eddy 2, at 19 March 2003 for Eddy 3, at 16 July 2003 for Eddy 4, at 3 September 2003 for Eddy 5 and at 5 May 2004 for Eddy 6. The SLA is in color and SST contours are at every degree.

OSD
11, 2367–2389, 2014

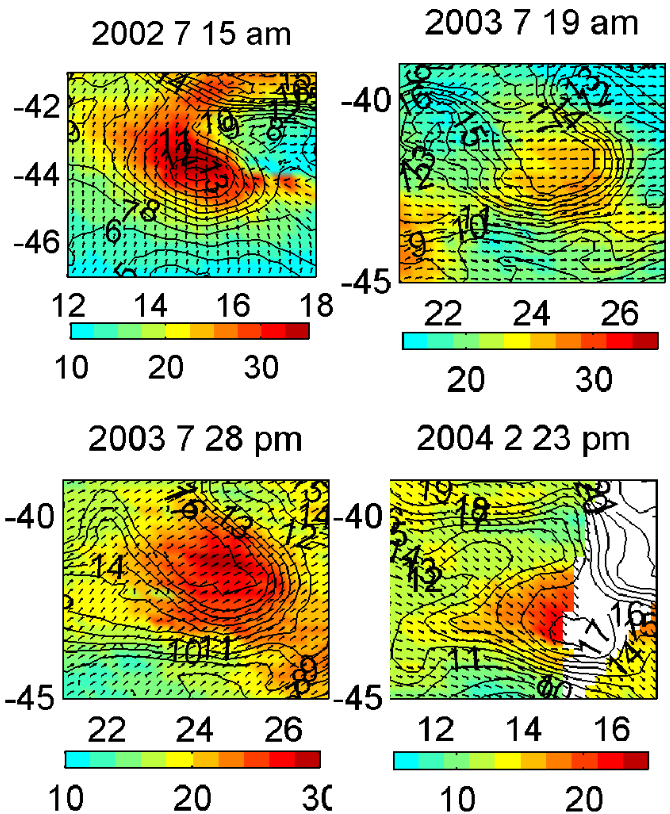

Figure 3. Clockwise from top left, Instantaneous estimate of QuikScat wind speed in $m\,s^{-1}$ (color) and directions (arrows) and AMSR microwave sea surface temperature (contours) south of the Agulhas Current system in the "Roaring forties" on the 15 July 2002 (morning path) 19 July 2003 (morning path), 23 February 2004 (evening path) and 28 July 2003 (evening path) showing strong and homogeneous increase and decrease in wind speed collocated with increases and decrease of sea surface temperature.

OSD
11, 2367–2389, 2014

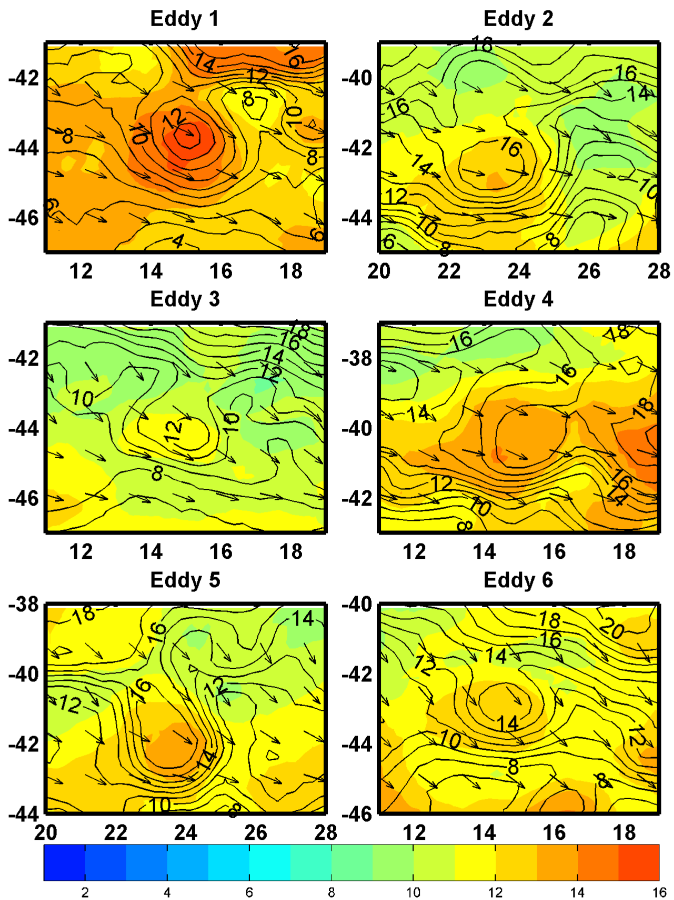

Figure 4. Mean weekly wind speeds (color) and directions (arrows) and SST (contours) above the six eddies. Times given correspond to weekly means centered at 10 July 2002 for Eddy 1, at 4 September 2002 for Eddy 2, at 19 March 2003 for Eddy 3, at 16 July 2003 for Eddy 4, at 3 September 2003 for Eddy 5 and at 5 May 2004 for Eddy 6.

OSD
11, 2367–2389, 2014

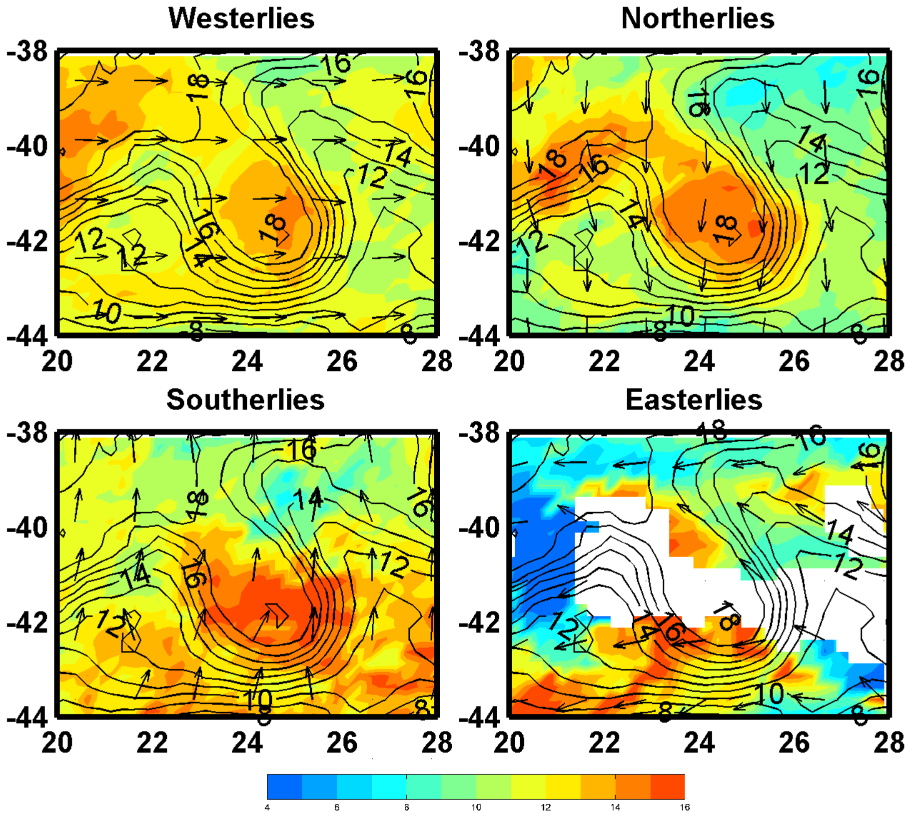

Figure 5. Mean wind speeds (color) and directions (arrows) and SST (contours) above eddy 5, estimated from twice daily QuikScat wind estimates for westerly (36 cases), northerly (18), easterly (1) and southerly wind (6) during July 2003 showing that wind increases for all direction.

OSD
11, 2367–2389, 2014

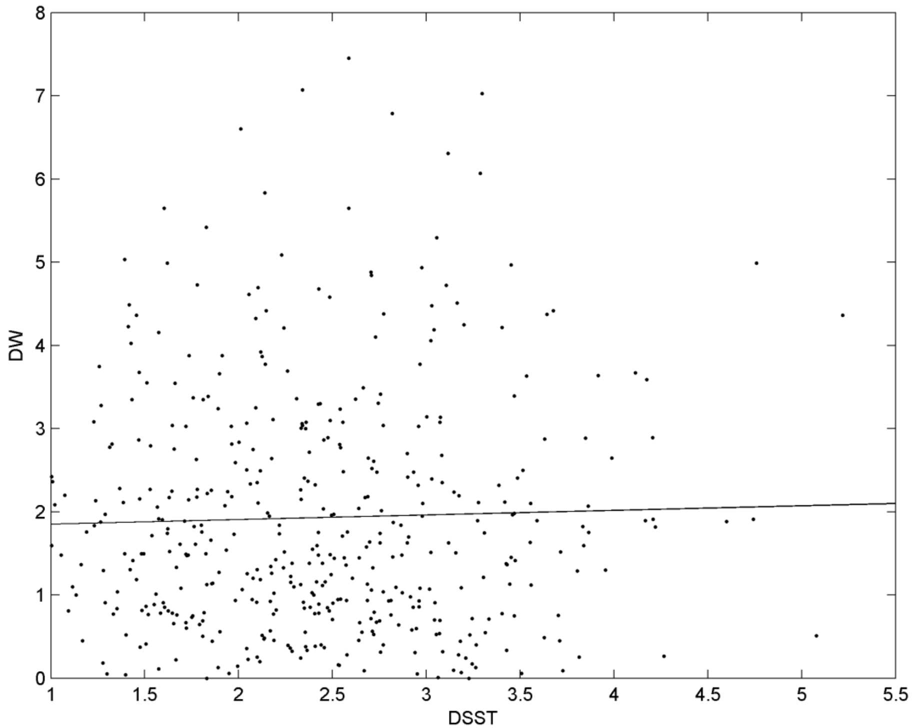

Figure 6. Scatter plot of SST perturbation (DSST) vs. wind speed increase (DW) for cases when the wind increased homogeneously above the all eddy and for SST perturbation for the surrounding ocean > 1 °C.

OSD
11, 2367–2389, 2014